optica

Quantum metrology at the limit with extremal Majorana constellations

F. Bouchard,[1] P. de la Hoz,[2] G. Björk,[3] R. W. Boyd,[1,4] M. Grassl,[5] Z. Hradil,[6] E. Karimi,[1,7,*] A. B. Klimov,[8] G. Leuchs,[5,1] J. Řeháček,[6] and L. L. Sánchez-Soto[2,5]

[1]Department of Physics, University of Ottawa, 150 Louis Pasteur, Ottawa, Ontario K1N 6N5, Canada
[2]Department of Optics, Faculty of Physics, Universidad Complutense, 28040 Madrid, Spain
[3]Department of Applied Physics, Royal Institute of Technology (KTH), AlbaNova, SE-106 91 Stockholm, Sweden
[4]Institute of Optics, University of Rochester, Rochester, New York 14627, USA
[5]Max Planck Institute for the Science of Light, Staudtstraß e 2, 91058 Erlangen, Germany
[6]Department of Optics, Palacký University, 17. listopadu 12, 771 46 Olomouc, Czech Republic
[7]Department of Physics, Institute for Advanced Studies in Basic Sciences, 45137-66731 Zanjan, Iran
[8]Department of Physics, Universidad de Guadalajara, 44420 Guadalajara, Jalisco, Mexico
*Corresponding author: ekarimi@uottawa.ca

Received 30 June 2017; revised 2 October 2017; accepted 21 October 2017 (Doc. ID 301465); published 17 November 2017

Quantum metrology allows for a tremendous boost in the accuracy of measurement of diverse physical parameters. The estimation of a rotation constitutes a remarkable example of this quantum-enhanced precision. The recently introduced Kings of Quantumness are especially germane for this task when the rotation axis is unknown, as they have a sensitivity independent of that axis and they achieve a Heisenberg-limit scaling. Here, we report the experimental realization of these states by generating up to 21-dimensional orbital angular momentum states of single photons, and confirm their high metrological abilities.

OCIS codes: (270.0270) Quantum optics; (270.5585) Quantum information and processing; (120.3940) Metrology.

https://doi.org/10.1364/OPTICA.4.001429

The conventional description of the quantum world involves a key mathematical object—the quantum state—that conveys complete information about the system under study; once it is known, the probabilities of the outcomes of any measurement can be predicted. This statistical description entails counterintuitive effects that have prompted several notions of quantumness, yet no single one captures the whole breadth of the physics.

There are, however, instances of quantum states that behave in an almost classical way. The paradigm of such a behavior is that of coherent states of light [1]; they are as much localized as possible in phase space, a property that is preserved under free evolution.

The concept of coherent states has been extended to other physical systems [2]. The case of spin is of paramount importance. The corresponding spin coherent states have minimal uncertainty and they are conserved under rotations. So, in the usual way of speaking, they mimic a classical angular momentum as much as possible. One could rightly wonder what kind of state might serve as the opposite of a coherent state. The answer will depend on the ways to formalize the idea of being "the opposite" [3]. Here, we take advantage of the Majorana representation, which maps a pure spin S into $2S$ points on the Bloch sphere [4].

It turns out that the Majorana representation of a coherent state consists of a single point (with multiplicity $2S$). At the opposite extreme, we can imagine states whose Majorana representations are spread uniformly over the sphere. The resulting states are precisely the Kings of Quantumness [5,6]. With such symmetric spreadings, the constellations essentially map onto themselves for relatively small rotations around arbitrary axes. This means that they resolve rotations around any axis approximately equally well. We emphasize that the problem of estimating a rotation is of utmost interest in magnetometry [7–9], polarimetry [10,11], and metrology in general [12]. In this work, we experimentally demonstrate the generation of these states and certify their potential for quantum metrology [13].

Let us first set the stage for our experiment. We consider a system that can be described in terms of two independent bosonic modes with creation operators $\hat{a}_\alpha^\dagger$, with $\alpha \in \{+,-\}$. This encompasses many different instances, such as strongly correlated systems, light polarization, Bose–Einstein condensates, and Gaussian–Schell beams, to mention only a few [14]. The Stokes operators for these two-mode systems can be compactly expressed as [15] $\hat{\mathbf{S}} = \frac{1}{2}\hat{a}_\alpha^\dagger \boldsymbol{\sigma}_{\alpha\beta}\hat{a}_\beta$, where $\boldsymbol{\sigma}$ denotes the Pauli matrices, and summation over repeated indices is assumed. One can verify that $\hat{\mathbf{S}}^2 = \hat{S}_0(\hat{S}_0+1)$ with $\hat{S}_0 = \hat{N}/2$, and $\hat{N} = \hat{a}_\alpha^\dagger \delta_{\alpha\beta}\hat{a}_\beta = \hat{N}_+ + \hat{N}_-$ being the total number of excitations.

From now on, we restrict our attention to the case where N is fixed. This corresponds to working in a $(2S+1)$-dimensional Hilbert space $\mathcal{H}_S$ of spin S (with $N = 2S$). This space $\mathcal{H}_S$ is spanned by the Dicke basis $|S, m\rangle$, wherein the action of $\hat{\mathbf{S}}$ operators is the standard for an angular momentum. Sometimes, it is preferable to use the two-mode Fock basis $|N_+, N_-\rangle$, related to the Dicke basis by $N_+ = S + m$ and $N_- = S - m$.

Spin coherent states are constructed much in the same way as in the canonical case [2]: they are displaced versions of the north pole of the Bloch unit sphere $\mathcal{S}_2$. If $\mathbf{n}$ is a unit vector in the direction of the spherical angles (θ, ϕ), they can be defined as $|\mathbf{n}\rangle = e^{i\phi\hat{S}_z}e^{i\theta\hat{S}_y}|S, S\rangle$. They are not orthogonal, but one can still decompose an arbitrary state $|\Psi\rangle$ using this overcomplete set. The associated coherent-state wave function is $\Psi(\mathbf{n}) = \langle\mathbf{n}|\Psi\rangle$, and the corresponding probability distribution, $Q(\mathbf{n}) = |\Psi(\mathbf{n})|^2$, is nothing but the Husimi function.

The wave function $\Psi(\mathbf{n})$ can be expanded in terms of the Dicke basis $|S, m\rangle$. If the corresponding coefficients are $\Psi_m = \langle S, m|\Psi\rangle$, we obtain $\Psi(\mathbf{n}) = (1+|z|^2)^{-S}\sum_{m=-S}^{S} c_m \Psi_m z^{S+m}$, where $c_m = \sqrt{(2S)!/[(S-m)!(S+m)!]}$, and $z = \tan(\theta/2)e^{-i\phi}$ is the complex number derived by the stereographic projection of (θ, ϕ). Apart from the unessential positive prefactor, this is a polynomial of order $2S$; thus, $|\Psi\rangle$ is determined by the set $\{z_i\}$ of the $2S$ complex zeros of $\Psi(\mathbf{n})$. These zeros, which are also the zeros of $Q(\mathbf{n})$, specify the so-called constellation by an inverse stereographic map of $\{z_i\} \mapsto (\theta_i, \phi_i)$.

Since the spherical harmonics $Y_{\mathrm{Kq}}(\mathbf{n})$ are a complete set of orthonormal functions on $\mathcal{S}_2$, they may be used to expand the Husimi function $Q(\mathbf{n})$. The resulting coefficients, ϱ_{Kq}, are nothing but the standard state multipoles [16], and there are $2S + 1$ of them (see Supplement 1). The monopole is trivial, as it is just a constant term. The dipole indicates the position of the state in the Bloch sphere. When it vanishes, the state has vanishing (first-order) polarization and points nowhere in the mean. If the quadrupole also vanishes, the variance of the state is uniform; i.e., no directional signature can be observed in its second-order fluctuations, and we say that it is second-order unpolarized. Similar interpretation holds for higher-order multipoles. One can also look at these multipoles as the Kth directional moments of the state constellation and, therefore, these terms resolve progressively finer angular features.

The quantity $\sum_q |\varrho_{\mathrm{Kq}}|^2$ gauges the overlap of the state with the Kth multipole pattern. It seems thus suitable to look at the cumulative distribution [17] $\mathcal{A}_M = \sum_{K=1}^{M}\sum_{q=-K}^{K}|\varrho_{\mathrm{Kq}}|^2$, which concisely condenses the state angular capacity up to order M $(1 \le M \le 2S)$. Observe that the monopole is omitted, as it is just a constant term.

The spin coherent states $|\mathbf{n}\rangle$ have remarkably simple constellations, just the point $-\mathbf{n}$, and they maximize $\mathcal{A}_M$ for all orders M, confirming yet from another perspective the outstanding properties of these states [5].

In contradistinction, the Kings are those pure states that make $\mathcal{A}_M \equiv 0$ for the highest possible value of M. This means that they convey the relevant information in higher-order fluctuations. The search for these states has been systematically undertaken recently in Ref. [5], where the interested reader can check the details (see also Supplement 1, where one can find the nonzero components Ψ_m of the Kings). The resulting Majorana constellations for some values of S are depicted in Fig. 1. For $S = 3$, the constellation is a regular octahedron and the state is third-order unpolarized $(M = 3)$. For $S = 5$, it consists of two pentagons. For $S = 6$ we have the icosahedron, and the corresponding state is fifth-order unpolarized. For $S = 10$ we have a slightly stretched dodecahedron (i.e., the four pentagonal rings that define its vertices are displaced against the pole), and it is fifth-order unpolarized. As we can appreciate, the Kings have the points very symmetrically placed on the unit sphere, so their constellations possess many axes along which they return to themselves after a rotation. Consequently, they can resolve relatively small angles around a large number of axes.

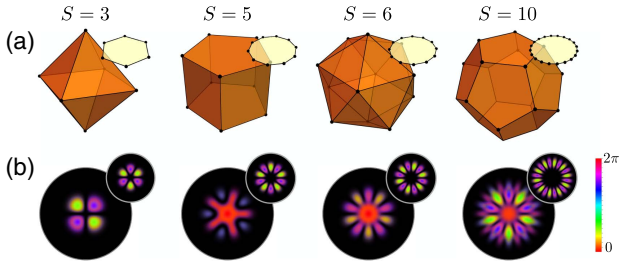

Fig. 1. (a) The Majorana constellations in the Bloch sphere for the Kings (orange) and the NOON states (yellow) corresponding to spin $S = 3$, 5, 6, and 10. (b) The Laguerre–Gauss representation of the same Kings and NOON states, shown in (a), where the azimuthal index ℓ corresponds to m in the Dicke basis. We consider the fundamental radial mode, i.e., $p = 0$, where p is the radial index of the Laguerre–Gauss modes.

Other states with a high degree of angular resolution are the NOON states, given by $|\mathrm{NOON}\rangle = \frac{1}{\sqrt{2}}(|N, 0\rangle - |0, N\rangle)$ in the two-mode Fock basis and $\frac{1}{\sqrt{2}}(|S, S\rangle - |S, -S\rangle)$ in the Dicke basis. As shown in Fig. 1, their Majorana constellation consists of $2S$ equidistantly placed points around the equator of $\mathcal{S}_2$. A rotation around the z axis of angle $\pi/(2S)$ makes $|\mathrm{NOON}\rangle$ orthogonal to itself, whereas for π/S it returns to itself. This nicely supports the ability of NOON states to detect small rotations.

To compare the performance of these two classes of states, let us assume we have to estimate a rotation $R(\omega, \mathbf{u})$ of angle ω around an axis $\mathbf{u}$ of spherical angles (Θ, Φ). We consider only small rotations and take the measurement to be a projection of the rotated state onto the original one; i.e., it can be represented by $\hat{P} = |\Psi\rangle\langle\Psi|$. As discussed in Supplement 1, the respective sensitivities (defined as the ratio $\Delta\omega = \Delta\hat{P}/|\partial\langle\hat{P}\rangle/\partial\omega|$, the variance being $\Delta\hat{P} = [\langle\hat{P}^2\rangle - \langle\hat{P}\rangle^2]^{1/2}$) are

$$\Delta\omega_{\mathrm{Kings}} = \frac{\sqrt{3}}{2}\frac{1}{\sqrt{S(S+1)}},$$
$$\Delta\omega_{\mathrm{NOON}} = \frac{1}{\sqrt{2}}\frac{1}{\sqrt{2S^2\cos^2\Theta + S\sin^2\Theta}}. \quad (1)$$

The sensitivity of the Kings is completely independent of the rotation axis and with a Heisenberg-limit scaling $1/S$ for large S. For the NOON states, the sensitivity scales as $1/S$ when $\Theta = 0$, but can be as bad as $1/\sqrt{S}$ when $\Theta = \pi/2$. In short, it is essential to know the rotation axis to ensure that the NOON state is aligned to achieve its best sensitivity.

We stress that the measurement scheme for $\Delta\omega$ involves only second-order moments of $\hat{\mathbf{S}}$. Given their properties, one could expect that detecting higher-order moments will bring out even more advantages of the Kings.

To check these issues, we have generated these extremal states for the cases of $S = 3$, 5, 6, and 10 using orbital angular momentum (OAM) states of single photons [18], which has already proven fruitful in quantum metrology [19]. Working at the single-photon regime is not essential, but it highlights the potential implications for quantum information processing [20]. Therefore, the index m in the Dicke basis is identified with the OAM eigenvalue ℓ of a single photon along its propagation

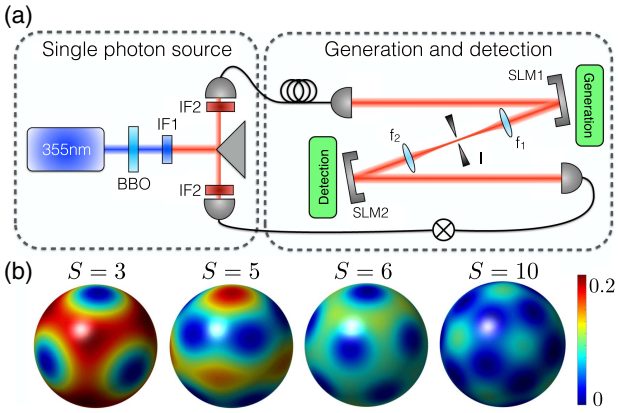

Fig. 2. (a) Sketch of the experimental setup and (b) density plots of the experimentally reconstructed Husimi Q functions for the same King states as in Fig. 1. The fidelities of these reconstructed states are (from left to right) 0.94, 0.87, 0.91, and 0.93. The differences with the theoretical Q functions cannot be visually noticed.

direction. In general, there exist many families of optical modes carrying OAM, but we choose the Laguerre–Gauss basis $\mathrm{LG}_{\ell,p}$, where p is the radial index. Since the radial profile is irrelevant to the experimental realization of the Kings states, for the sake of simplicity, we always set the radial index to its fundamental value, i.e., $p = 0$. The resulting transverse profiles of both the Kings and the NOON states are as in Fig. 1(b).

We experimentally create the Kings by means of spontaneous parametric downconversion. A sketch of the experimental setup is shown in Fig. 2(a). A quasi-continuous wave ultraviolet (UV) laser operating with a repetition rate of 100 MHz and an average power of 150 mW at a wavelength of 355 nm is used to pump a type-I β-barium borate crystal. The single photons, signal and idler, are subsequently coupled to single-mode fibers to filter their spatial mode. One of the photons, the idler, is used as a trigger. The other photon, the signal, is made incident on a first spatial light modulator (SLM1), where the desired quantum states were imprinted on the signal photon holographically [21]. The generated photonic Kings are subsequently imaged onto a second spatial light modulator (SLM2) by a $4f$ system. The second SLM possessing the desired hologram followed by a single-mode optical fiber perform the projective measurement on the state of the signal photon. Both photons are sent to avalanche photodiode detectors (APD), and coincidence counts are recorded by a coincidence box with a coincidence time window of 3 ns [22].

To verify the accurate experimental generation of these states, we perform quantum state tomography to reconstruct the Husimi Q function, as shown in Fig. 2(b). The average fidelity of the resulting states is around 90%; i.e., 94%, 87%, 91%, and 93%, respectively (see Supplement 1).

We now study the behavior of such states under rotations in the sphere $\mathcal{S}_2$. This is experimentally realized by projective measurements of the Kings onto themselves after a rotation ω around several axes (see Fig. 3). To demonstrate the high sensitivity to rotation of these states along arbitrary axes, we perform such rotations around each axis passing through the Majorana points and facets of the Kings constellations. For the cases of $S = 3$, 6, and 10, we find four-, five-, and three-fold symmetry axes passing through their Majorana points and three-, three-, and five-fold symmetry axes passing through the normals to the facets of their constellations, respectively. Note that, since we are dealing with OAM, these rotations correspond to rather abstract mode transformations, although the polar axis still represents a physical real-space rotation around the optical axis.

Finally, in Fig. 4 we experimentally check the sensitivity of the Kings and NOON states. As we can see, the experimental

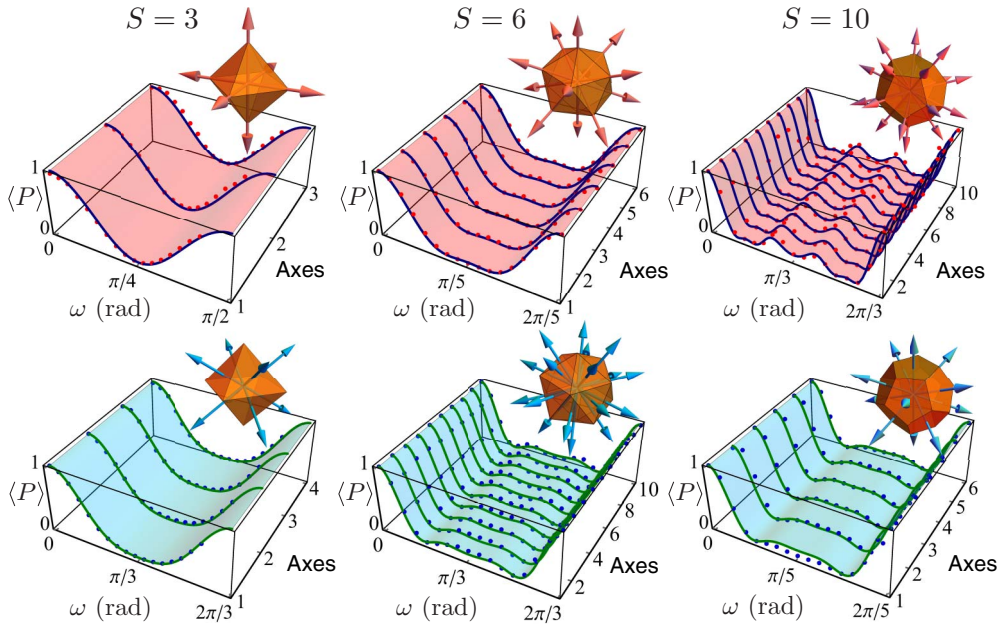

Fig. 3. Experimental results of the projection of the $S = 3$, 6, and 10 (first, second, and third column, respectively) Kings states, $|\Psi^{(S)}\rangle$, onto themselves after a rotation of ω around the axis $\mathbf{u}$, $\hat{R}(\omega, \mathbf{u})$, i.e., $\langle\hat{P}\rangle = |\langle\Psi^{(S)}|\hat{R}(\omega, \mathbf{u})|\Psi^{(S)}\rangle|^2$. The axes are presented graphically along with the associated constellations. The first row corresponds to rotations along the axes passing through the Majorana points (pink arrows), and the second row corresponds to rotations along the axes normal to the facets of the constellations (blue arrows). The experimental results (red and blue dots) are shown along with the theoretical results (blue and green curves) for all rotation axes.

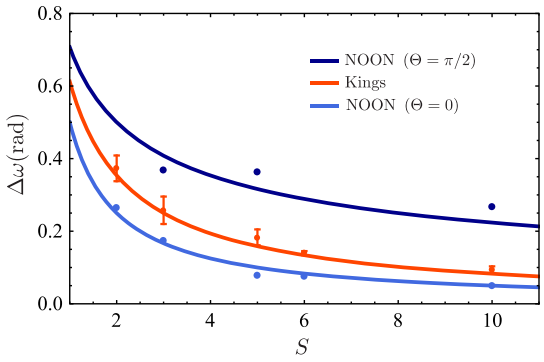

Fig. 4. Rotational sensitivity $\Delta\omega$ for the Kings (red) and NOON states (blue). The solid curves correspond to the theory predicted in Eq. (1), and the points correspond to experimental results. In the case of the Kings, we show the mean rotational sensitivity over all axes presented in Fig. 3, where the error bars correspond to variation in sensitivity from axes to axes. For the NOON states, we show the rotational sensitivity for rotation axes with $\Theta = 0$ and $\Theta = \pi/2$.

sensitivity of the Kings is completely independent of the orientation of the rotation axes (within the error bars). In the limit of small rotation angles, the NOON states overcome the Kings all the way up to $\cos\Theta = 1/\sqrt{3}$. Nonetheless, since the Kings achieve the ideal sensitivity irrespectively of the axis, they are the most appropriate to detect rotation around arbitrary axes.

The problem of the Kings is closely related to other notions as states of maximal Wehrl–Lieb entropy [23], Platonic states [24], the Queens of Quantumness [25], or the Thomson problem [26]. However, there are still many things to elucidate concerning these links. They are, however, a nice illustration of the connections between different branches of science, and on how some seemingly simple problems—distributing points in the most symmetric manner on a sphere—can illuminate such complicated optimization problems that we have just described.

Thus far, efforts were concentrated in estimating the rotation angle, which in terms of magnetometry means that we only want to know the magnetic field magnitude. The Kings will allow for a simultaneous precise determination of the rotation axis (i.e., the magnetic field direction). Our experimental results corroborate that this extra advantage can pave the way to much more refined measurement schemes.

Funding. Natural Sciences and Engineering Research Council of Canada (NSERC); Canada Foundation for Innovation (CFI); Technologická Agentura České Republiky (TAČR) (TE01020229); Grantová Agentura České Republiky (GACR) (15-03194S); Ministerio de Economía y Competitividad (MINECO) (FIS2015-67963-P).

Acknowledgment. F. B. acknowledges the support of the Vanier Canada Graduate Scholarships Program of the Natural Sciences and Engineering Research Council of Canada (NSERC). E. K. acknowledges the support of the Canada Research Chairs (CRC), and Canada Foundation for Innovation (CFI) Programs. F. B., R. W. B., and E. K. acknowledge the support of the Max Planck–University of Ottawa Centre for Extreme and Quantum Photonics. G. B. acknowledges the support of the Wenner–Gren Foundation and the Swedish Research Council (VR) through the Linnaeus Center of Excellence ADOPT.

See Supplement 1 for supporting content.

REFERENCES

1. R. J. Glauber, Phys. Rev. **131**, 2766 (1963).
2. A. Perelomov, *Generalized Coherent States and Their Applications* (Springer, 1986).
3. J. Zimba, Electron. J. Theor. Phys. **3**, 143 (2006).
4. E. Majorana, Nuovo Cimento **9**, 43 (1932).
5. G. Björk, A. B. Klimov, P. de la Hoz, M. Grassl, G. Leuchs, and L. L. Sánchez-Soto, Phys. Rev. A **92**, 031801 (2015).
6. G. Björk, M. Grassl, P. de la Hoz, G. Leuchs, and L. L. Sánchez-Soto, Phys. Scripta **90**, 108008 (2015).
7. W. Wasilewski, K. Jensen, H. Krauter, J. J. Renema, M. V. Balabas, and E. S. Polzik, Phys. Rev. Lett. **104**, 133601 (2010).
8. R. J. Sewell, M. Koschorreck, M. Napolitano, B. Dubost, N. Behbood, and M. W. Mitchell, Phys. Rev. Lett. **109**, 253605 (2012).
9. W. Muessel, H. Strobel, D. Linnemann, D. B. Hume, and M. K. Oberthaler, Phys. Rev. Lett. **113**, 103004 (2014).
10. V. Meyer, M. A. Rowe, D. Kielpinski, C. A. Sackett, W. M. Itano, C. Monroe, and D. J. Wineland, Phys. Rev. Lett. **86**, 5870 (2001).
11. V. D'Ambrosio, N. Spagnolo, L. Del Re, S. Slussarenko, Y. Li, L. C. Kwek, L. Marrucci, S. P. Walborn, L. Aolita, and F. Sciarrino, Nat. Commun. **4**, 2432 (2013).
12. L. A. Rozema, D. H. Mahler, R. Blume-Kohout, and A. M. Steinberg, Phys. Rev. X **4**, 041025 (2014).
13. V. Giovannetti, S. Lloyd, and L. Maccone, Nat. Photonics **5**, 222 (2011).
14. S. Chaturvedi, G. Marmo, and N. Mukunda, Rev. Math. Phys. **18**, 887 (2006).
15. A. Luis and L. L. Sánchez-Soto, Prog. Opt. **41**, 421 (2000).
16. K. Blum, *Density Matrix Theory and Applications* (Plenum, 1981).
17. P. de la Hoz, A. B. Klimov, G. Björk, Y. H. Kim, C. Müller, C. Marquardt, G. Leuchs, and L. L. Sánchez-Soto, Phys. Rev. A **88**, 063803 (2013).
18. L. Allen, S. M. Barnett, and M. J. Padgett, *Optical Angular Momentum* (Institute of Physics, 2003).
19. D. S. Simon, G. Jaeger, and A. V. Sergienko, *Quantum Metrology, Imaging, and Communication* (Springer, 2017).
20. J. Leach, M. J. Padgett, S. M. Barnett, S. Franke-Arnold, and J. Courtial, Phys. Rev. Lett. **88**, 257901 (2002).
21. E. Bolduc, N. Bent, E. Santamato, E. Karimi, and R. W. Boyd, Opt. Lett. **38**, 3546 (2013).
22. H. Qassim, F. M. Miatto, J. P. Torres, M. J. Padgett, E. Karimi, and R. W. Boyd, J. Opt. Soc. Am. B **31**, A20 (2014).
23. A. Baecklund and I. Bengtsson, Phys. Scripta **T163**, 014012 (2014).
24. P. Kolenderski and R. Demkowicz-Dobrzanski, Phys. Rev. A **78**, 052333 (2008).
25. O. Giraud, P. Braun, and D. Braun, New J. Phys. **12**, 063005 (2010).
26. J. J. Thomson, Philos. Mag. **7**(39), 237 (1904).

optica

Quantum metrology at the limit with extremal Majorana constellations: supplemental material

F. Bouchard[1], P. de la Hoz[2], G. Björk[3], R. W. Boyd[1,4], M. Grassl[5], Z. Hradil[6], E. Karimi[1,7], A. B. Klimov[8], G. Leuchs[5,1], J. Řeháček[6], and L. L. Sánchez-Soto[2,5,*]

[1]Department of Physics, University of Ottawa, 150 Louis Pasteur, Ottawa, Ontario, K1N 6N5 Canada
[2]Department of Optics, Faculty of Physics, Universidad Complutense, 28040 Madrid, Spain
[3]Department of Applied Physics, Royal Institute of Technology (KTH), AlbaNova, SE-106 91 Stockholm, Sweden
[4]Institute of Optics, University of Rochester, Rochester, New York, 14627, USA
[5]Max Planck Institute for the Science of Light, Staudtstraße 2, 91058 Erlangen, Germany
[6]Department of Optics, Palacký University, 17. listopadu 12, 771 46 Olomouc, Czech Republic
[6]Departamento de Óptica, Facultad de Física, Universidad Complutense, 28040 Madrid, Spain
[7]Department of Physics, Institute for Advanced Studies in Basic Sciences, 45137-66731 Zanjan, Iran
[8]Department of Physics, Universidad de Guadalajara, 44420 Guadalajara, Jalisco, Mexico
[*]Corresponding author: lsanchez@fis.ucm.es

Published 17 November 2017

This document provides supplementary information to "Quantum metrology at the limit with extremal Majorana constellations," https://doi.org/10.1364/OPTICA.4.001429.

https://doi.org/10.6084/m9.figshare.5533669

1. MULTIPOLES AND EXTREMAL STATES

We consider a state represented by a density matrix $\hat{\varrho}$ living in the $(2S+1)$-dimensional Hilbert space $\mathcal{H}_S$ of spin S. The state multipoles can be defined in terms of the Husimi Q function as

$$\varrho_{Kq} = C_K \int_{\mathcal{S}_2} d^2\mathbf{n}\, Y_{Kq}(\mathbf{n})\, Q(\mathbf{n})\,, \tag{1}$$

where the normalization constant is

$$C_K = \sqrt{\frac{4\pi}{2S+1}}\,\frac{1}{C^{SS}_{SS,K0}}\,, \tag{2}$$

and $C^{SS}_{SS,K0}$ is a Clebsch-Gordan coefficient [1].

When expressed in the Cartesian basis they appear in a very transparent way. For example, the three dipole (ϱ_{1q}) and the five quadrupole (ϱ_{2q}) terms can be given, respectively, as

$$\wp_i = \langle n_i \rangle\,, \qquad \mathcal{Q}_{ij} = \langle 3n_i n_j - \delta_{ij} \rangle\,, \tag{3}$$

where $\langle f(\mathbf{n})\rangle = \int_{\mathcal{S}_2} d^2\mathbf{n}\, f(\mathbf{n})\, Q(\mathbf{n}) / \int_{\mathcal{S}_2} d^2\mathbf{n}\, Q(\mathbf{n})$ and the index i runs x, y, and z. These multipoles appear then as the standard ones in electrostatics, but replacing the charge density by $Q(\mathbf{n})$ and distances by directions [2]. It is also clear that they are the Kth directional moments of the state constellation and, therefore, these terms resolve progressively finer angular features.

We look at the cumulative distribution

$$\mathcal{A}_M = \sum_{K=1}^{M} \sum_{q=-K}^{K} |\, \varrho_{Kq}\,|^2\,, \tag{4}$$

which sums polarization information up to order M ($1 \leq M \leq 2S$). The distribution $\mathcal{A}_M$ can be regarded as a nonlinear functional of the density matrix $\hat{\varrho}$. On that account, one can try to ascertain the states that maximize $\mathcal{A}_M$ for each order M. As with any cumulative distribution, $\mathcal{A}_M$ is a monotonically nondecreasing function of the multipole order. We shall be considering only pure states, which we expand in the Dicke basis as $|\Psi\rangle = \sum_{m=-S}^{S} \Psi_m\, |S, m\rangle$, with coefficients $\Psi_m = \langle S, m|\Psi\rangle$. We easily get

$$\mathcal{A}_M = \sum_{K=1}^{M} \sum_{q=-K}^{K} \frac{2K+1}{2S+1} \left| \sum_{m,m'=-S}^{S} C^{Sm'}_{Sm,Kq}\, \Psi_{m'} \Psi^*_m \right|^2 . \tag{5}$$

As it has been proven in Ref. [3], spin coherent states $|\mathbf{n}\rangle$ maximize $\mathcal{A}_M$ for all orders M.

We concentrate on the opposite case of states minimizing $\mathcal{A}_M$. Obviously, the maximally mixed state

$$\hat{\varrho} = \frac{1}{2S+1}\hat{\mathbb{1}}_{2S+1} \tag{6}$$

kills all the multipoles and so indeed causes Eq. (4) to vanish for all M, being fully unpolarized [4, 5]. Nonetheless, we are interested in pure Mth-order unpolarized states. The strategy we adopt is thus very simple to state: starting from a set of unknown normalized state amplitudes in Eq. Eq. (5), which we write as $\Psi_m = a_m + ib_m$ ($a_m, b_m \in \mathbb{R}$), we try to get $\mathcal{A}_M = 0$ for the highest possible M. This yields a system of polynomial equations of degree two for a_m and b_m, which we solve using Gröbner bases implemented in the computer algebra system MAGMA. In this way, we get exact algebraic expressions and we can detect when there is no feasible solution.

The detailed list of resulting minimal states, which are the Kings of Quantumness, can be found in [6], where the reader can also see the associated Majorana constellations. In this paper, we have considered the cases of $S = 3, 5, 6$ and 10: the Kings have the following nonzero Ψ_m components:

$$\begin{array}{l|lll} S=3 & \Psi_{\pm 2} = \mp\frac{1}{\sqrt{2}} & & \\ S=5 & \Psi_{\pm 5} = \frac{1}{\sqrt{5}} & \Psi_0 = \sqrt{\frac{3}{5}} & \\ S=6 & \Psi_{\pm 5} = \mp\frac{\sqrt{7}}{5} & \Psi_0 = \frac{\sqrt{11}}{5} & \\ S=10 & \Psi_{\pm 10} = \frac{\sqrt{561}}{75} & \Psi_{\pm 5} = \mp\frac{3\sqrt{209}}{75} & \Psi_0 = \frac{\sqrt{741}}{75} \end{array} \tag{7}$$

Intuitively, these constellations seem to have the points as symmetrically placed on the unit sphere as possible. We have explored the connection with spherical t-designs [7], which are patterns of N points on a sphere such that every polynomial of degree at most t has the same average over the N points as over the sphere. Thus, the N points mimic a flat distribution up to order t, which obviously implies a fairly symmetric distribution.

For a given S, the maximal order of M for which we can cancel out $\mathcal{A}_M$ does not follow a clear pattern. However, the numerical evidence suggests that $M_{\max}$ coincides with $t_{\max}$ in the corresponding spherical design. Further work is needed, however, to support this conjecture.

2. ROTATIONAL SENSITIVITY

The goal of our work is the estimation of a rotation $\hat{R}(\omega, \mathbf{u})$ of angle ω around an axis $\mathbf{u}$ of spherical angles (Θ, Φ); i.e.,

$$\hat{R}(\omega, \mathbf{u}) = \exp(-i\omega\, \hat{S}\cdot\mathbf{u})\,, \tag{8}$$

which is generated precisely by $\hat{S}\cdot\mathbf{u}$. Our measurement was a projection onto the original state; i.e., $\hat{P} = |\Psi\rangle\langle\Psi|$. The sensitivity of the state $|\Psi\rangle$ to this measurement can be retrieved from a simple error propagation [8]

$$\Delta\omega = \frac{\Delta\hat{P}}{\left|\partial\langle\hat{P}\rangle/\partial\omega\right|}\,, \tag{9}$$

where the variance is $\Delta\hat{P} = [\langle\hat{P}^2\rangle - \langle\hat{P}\rangle^2]^{1/2}$. Note that for projective measurements, we have the simplification $\Delta\hat{P} = [\langle\hat{P}\rangle - \langle\hat{P}\rangle^2]^{1/2}$, and so the knowledge of $\langle\hat{P}\rangle$ is enough to assess $\Delta\omega$.

We consider only small rotations, which means that the angle ω is small enough to expand $\hat{R}(\omega, \mathbf{u})$ up to second order. Obviously, $\langle\hat{P}\rangle = |\langle\Psi|\hat{R}|\Psi\rangle|^2$ and then, after a direct computation, we get

$$\langle\hat{P}\rangle = \left|1 - i\omega\,\langle\hat{S}\rangle\cdot\mathbf{u} - \tfrac{1}{2}\omega^2\langle(\hat{S}\cdot\mathbf{u})^2\rangle\right|^2\,. \tag{10}$$

The last term is a little messy, but can be evaluated; the result reads (after expanding up to ω^2 and using spherical coordinates)

$$\langle\hat{P}_{\text{Kings}}\rangle = 1 - \frac{1}{3}\omega^2 S(S+1)\,, \tag{11}$$

$$\langle\hat{P}_{\text{NOON}}\rangle = 1 - \frac{1}{2}\omega^2 S\left(\sin^2\Theta + 2S\cos^2\Theta\right)\,. \tag{12}$$

From here we can finally get the sensitivity

$$\Delta\omega_{\text{Kings}} = \frac{\sqrt{3}}{2}\frac{1}{\sqrt{S(S+1)}}\,, \tag{13}$$

$$\Delta\omega_{\text{NOON}} = \frac{1}{\sqrt{2}}\frac{1}{\sqrt{2S^2\cos^2\Theta + S\sin^2\Theta}}\,, \tag{14}$$

as quoted in the Letter.

3. NOON STATES ROTATION

We experimentally generate our states using the OAM of single photons. In consequence, the index m in the Dicke basis is identified with the OAM eigenvalue ℓ of a single photon along its propagation direction. In this representation, only the azimuthal modes; i.e., $\exp(i\ell\phi)$, are relevant. In general, there exist many families of optical modes carrying OAM. Here, we choose the Laguerre-Gauss basis $\text{LG}_{\ell,p}$. As the radial profile is irrelevant to the experimental realization of the Kings states using OAM, for the sake of simplicity, we set the radial index to its fundamental value; i.e., $p = 0$.

The energy of modes with different azimuthal mode index ℓ varies slightly with the absolute value of the index. Thus a transformation of a state with predominant contribution of modes with large $|\ell|$ to one with a predominant contribution of modes with vanishing ℓ will result in a red-shift due to the rotational Doppler effect. However, for two reasons this effect will be miniscule. The first is that the wave-vector along the axis of propagation is much larger than the azimuthal wave vector. Secondly, the King state per definition comprises of points spread rather evenly on the Bloch sphere, thus involving modes with both small and large $|\ell|$. After a transformation, the points will still be rather evenly spread over the Bloch sphere (the constellation rotates rigidly), so while some of the constituent modes will get red-shifted, other will be blue-shifted. This will further act to hide any rotational Doppler shift.

In Fig. 1, we experimentally confirm the superiority of the Kings over the NOON states. For this purpose, we have used the case of $S = 3, 6$ and 10, as well. To compare the performances of the NOON states with that of the Kings, we perform the same set of projective measurements by rotating the NOON states over the same axes discussed in previously for the Kings. However, due to their lack of rotation sensitivity, the NOON states are studied under a full rotation of π. As it was expected, the NOON states possess the largest sensitivity to rotation for a single axis (z), thus overcoming the Kings for this case. Nonetheless, it is clearly evident that the Kings are distinctly superior with respect to any other rotation axes.

4. TOMOGRAPHIC RECONSTRUCTION

To verify the generated states two different sets of projections were utilized: (i) projections onto coherent states and (ii) projections onto rotated Kings with the axes of rotations defined

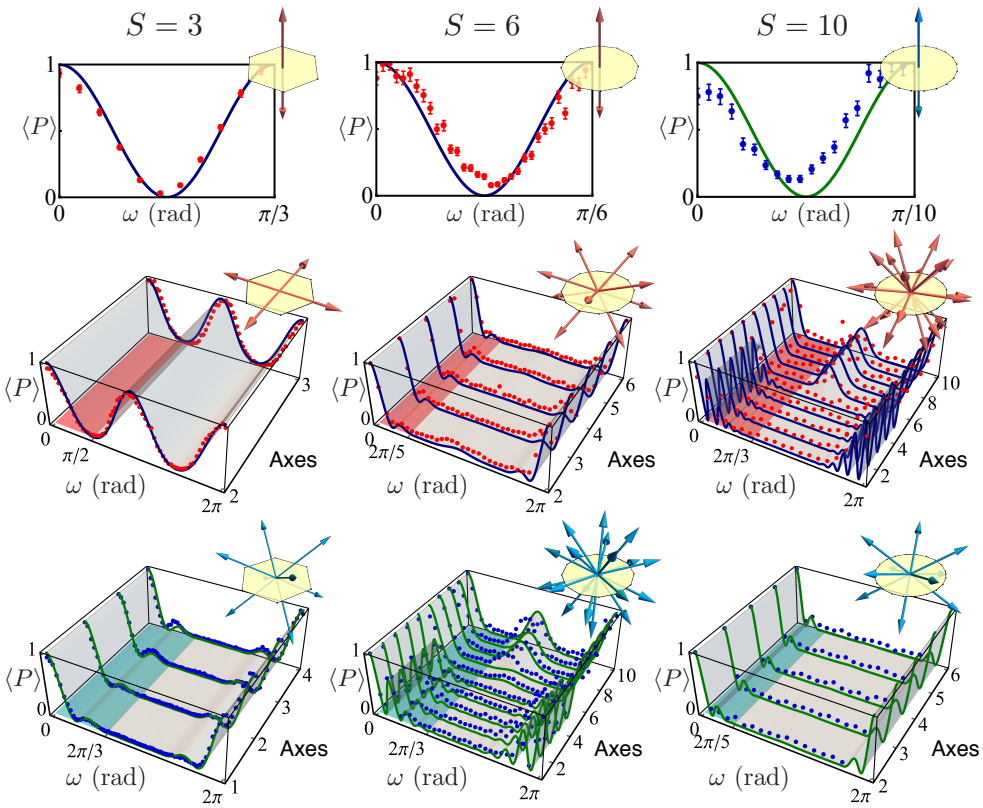

Fig. 1. Kings superiority over NOON states. Experimental results of projecting NOON states corresponding to $S = 3, 6$ and 10 onto themselves after a rotation along the various axes sketched in Fig. 3 of the main text. In the first row, the NOON states are rotated around their optimal z axis. For a comparison of the NOON versus the Kings, we show rotations of the NOON states along the axes of rotation defined by the Majorana points (second row) and the normal to the facets (third row) of the constellations of the Kings with corresponding S . The axes are presented graphically along with the associated constellations on the top-right corner of each plot. The coloured region (red for Majorana points rotations and blue for facets rotation) shows the region for which the Kings are mapped back onto themselves, as shown in Fig. 3 of the main text.

by the Majorana points. Such a D-dimensional channel can be described by an overcomplete positive operator-valued measurement (POVM) $\hat{\Pi}_j \geq 0, j = 1, \ldots, D$. The probabilities p_j of observed relative frequencies f_j, as given by the Born rule $p_j = \mathrm{Tr}(\hat{\varrho}\hat{\Pi}_j)$ can be inverted by maximizing the Fermi extended likelihood [9]

$$\mathcal{L} = \sum_j^D f_j \log\left(\frac{p_j}{\sum_{j'} p_{j'}}\right) \tag{15}$$

to yield the Kings estimates. This amounts to solving the extremal equation

$$\hat{R}\hat{\varrho} = \hat{G}\hat{\varrho}\,, \tag{16}$$

where we have defined

$$\hat{R} = \sum_j \frac{f_j}{p_j(\rho)}\hat{\Pi}_j, \qquad \hat{G} = \frac{\sum_j f_j}{\sum_j p_j(\rho)}\sum_j \hat{\Pi}_j. \tag{17}$$

This can be solved in an iterative way

$$\hat{\varrho}^{(k+1)} = \hat{G}^{-1}\hat{R}\hat{\varrho}^{(k)}\hat{R}\hat{G}^{-1}, \tag{18}$$

starting from the $(2S+1)$-dimensional maximally mixed state (6). A few thousand of iterations are typically needed to observe a convergence to the stationary point of the map Eq. (16).

In the experiment, several hundred of projections were recorded for each King and the fidelities of the estimated states with respect to the target states were found to be close to or in excess of 90% in all cases. See Table 1 for details.

The conventional description of the quantum world involves a key mathematical object—the quantum state—that conveys complete information about the system under study: once it is known, the probabilities of the outcomes of any measurement can be predicted. This statistical description entails many counterintuitive effects that have prompted several notions of quantumness, yet no single one captures the whole breadth of the physics.

S	dim	D	fidelity
3	7	288	0.94
5	11	572	0.87
6	13	544	0.91
10	21	1054	0.93

Table 1. Measurement sizes D and resulting fidelities obtained with quantum state tomography of experimentally generated King states.

REFERENCES

1. D. A. Varshalovich, A. N. Moskalev, and V. K. Khersonskii, *Quantum Theory of Angular Momentum* (World Scientific, Singapore, 1988).
2. J. D. Jackson, *Classical Electrodynamics* (John Wiley, New York, 1999), 3rd ed.
3. G. Björk, A. B. Klimov, P. de la Hoz, M. Grassl, G. Leuchs, and L. L. Sánchez-Soto, "Extremal quantum states and their Majorana constellations," Phys. Rev. A **92**, 031801 (2015).
4. H. Prakash and N. Chandra, "Density operator of unpolarized radiation," Phys. Rev. A **4**, 796–799 (1971).
5. G. S. Agarwal, "On the state of unpolarized radiation," Lett. Nuovo Cimento **1**, 53–56 (1971).
6. "http://polarization.markus-grassl.de," .
7. P. Delsarte, J. M. Goethals, and J. J. Seidel, "Spherical codes and designs," Geom. Dedicata **6**, 363–388 (1977).
8. A. K. Jha, G. S. Agarwal, and R. W. Boyd, "Supersensitive measurement of angular displacements using entangled photons," Phys. Rev. A **83**, 053829 (2011).
9. M. G. A. Paris and J. Řeháček, eds., *Quantum State Estimation*, vol. 649 of *Lect. Not. Phys.* (Springer, Berlin, 2004).